Supplementary Tables

Supplementary Table 1. Extracted 1D, 2D and 3D features. L is the sequence length.

Type	Name and shape	Description
1D	Nucleotide sequence $(L, 5)$	One-hot encoded base types for each nucleotide (4), and encoded relative position information in the sequence (1).
	backbone orientations $(L, 14)$	Seven backbone torsion angles: α, β, γ, δ, ε, ξ and χ; Represented using sine and cosine.
	Ultrafast Shape Recognition (USR)[1,2] $(L, 48)$	For each C4' atom, three sets of distances (from the current C4', from the C4' furthest from the current, and from the C4' furthest from the second reference) to all other C4' atoms are calculated. Each of these three distance sets is then encoded using Gaussian radial basis functions.
2D	inter-nucleotide distance $(L, L, 48)$	Three distance maps for each pair of nucleotides: P to P, C4' to C4', and glycosidic N to glycosidic N distance maps; Distances are encoded by Gaussian radial basis functions, respectively.
	Rosetta energies $(L, L, 9)$	Two-body terms in Rosetta: fa_atr, fa_rep, lk_nonpolar, rna_torsion, fa_stack, stack_elec, geom_sol_fast, hbond_sc, and fa_elec_rna_phos_phos
	Steric clashes $(L, L, 1)$	The frequency of pairwise non-hydrogen atomics clash: $$P_{\text{clash}}(M,N) = \frac{\sum_{m \in M}\sum_{n \in N} \mathrm{I}(d_{mn} < r_m + r_n - 0.4)}{\sum_{n \in N}\sum_{n \in N} 1}$$ The atomic radii for carbon (C), nitrogen (N), oxygen (O), and phosphorus (P) atoms are set as 1.7, 1.55, 1.52, and 1.8 Å, respectively
3D	nucleotide-level voxelization $(L, 3, 32, 32, 32)$	Each nucleotide is represented by a 3-channel (atomic occupation, mass, charge) voxelization of its atoms into a 32 × 32 × 32 Å grid, resulting in a (3, 32, 32, 32) feature map per nucleotide.[3]

Supplementary Table 2. Number of decoys per RNA target in T24 benchmark sets.

Method	Number of decoys per target
AlphaFold3[4]	5
DeepFoldRNA[5]	12
DRFold[6]	8
Molecular dynamics simulations	0~20*
RhoFold[7]	2
RNAComposer[8,9]	1
RoseTTAFold2NA[10]	2
Rosetta fragment assembly-based modeling	0~50**
trRosettaRNA[11]	5
SimRNA[12]	1
Structure perturbation	20
Total	35

* depending on the success of the MD simulations.

** depending on the number of available templates.

Supplementary Table 3. Performance on the test dataset T24. Values in **bold** indicate the best performance, while those with <u>underlines</u> represent the second-best. AUC was calculated on the overall data with an lDDT$_{RNA}$ cutoff of 75 to differentiate between 'good' and 'bad' decoys. $\rho_{lDDT(Global)}$, $\rho_{lDDT(Local)}$ and ρ_{RMSD} represent the Spearman correlation between the assessment scores and the true global lDDT$_{RNA}$, local lDDT$_{RNA}$, and RMSD, respectively. All correlation values are reported as absolute values.

Method	Overall				Per-target average				
	$\rho_{lDDT(Global)}$	$\rho_{lDDT(Local)}$	ρ_{RMSD}	AUC	$\rho_{lDDT(Global)}$	$\rho_{lDDT(Local)}$	ρ_{RMSD}	top 1 lDDT$_{RNA}$	top 1 RMSD(Å)
RNArank	**0.949**	**0.879**	**0.832**	**0.951**	**0.936**	**0.865**	**0.821**	**83.6**	**7.9**
lociPARSE	0.320	<u>0.314</u>	0.212	<u>0.858</u>	0.303	0.290	0.155	<u>76.9</u>	<u>9.2</u>
RNA3DCNN	<u>0.423</u>	0.279	<u>0.237</u>	0.805	0.457	<u>0.334</u>	0.312	57.5	14.5
DFIRE-RNA	0.108	-	0.221	0.642	0.650	-	0.520	68.5	12.9
cgRNASP	0.215	-	0.095	0.704	0.668	-	0.533	70.9	11.8
cgRNASP-PC	0.156	-	0.152	0.652	0.648	-	<u>0.550</u>	69.9	12.4
cgRNASP-C	0.234	-	0.098	0.698	<u>0.675</u>	-	0.534	66.7	13.2
rsRNASP	0.372	-	0.083	0.769	0.647	-	0.502	68.6	12.9
Ideal value	1	1	1	1	1	1	1	94.6	1.9

Supplementary Table 4. Performance on 12 CASP15 targets. Values in **bold** indicate the best performance, while those with <u>underlines</u> represent the second-best. AUC was calculated on the overall data with an lDDT$_{RNA}$ cutoff of 75 to differentiate between 'good' and 'bad' decoys. $\rho_{lDDT(Global)}$, $\rho_{lDDT(Local)}$ and ρ_{RMSD} represent the Spearman correlation between the assessment scores and the true global lDDT$_{RNA}$, local lDDT$_{RNA}$, and RMSD, respectively. All correlation values are reported as absolute values.

Method	Overall				Per-target average				
	$\rho_{lDDT(Global)}$	$\rho_{lDDT(Local)}$	ρ_{RMSD}	AUC	$\rho_{lDDT(Global)}$	$\rho_{lDDT(Local)}$	ρ_{RMSD}	top 1 lDDT$_{RNA}$	top 1 RMSD(Å)
RNArank	**0.706**	**0.589**	**0.686**	**0.915**	0.552	**0.536**	**0.395**	**67.0**	**14.3**
lociPARSE	<u>0.511</u>	<u>0.505</u>	0.200	0.673	**0.574**	<u>0.419</u>	0.304	<u>64.6</u>	<u>19.3</u>
RNA3DCNN	0.262	0.272	0.067	<u>0.685</u>	0.239	0.244	0.099	37.9	32.3
DFIRE-RNA	0.023	-	<u>0.534</u>	0.379	0.526	-	<u>0.352</u>	58.6	20.7
cgRNASP	0.096	-	0.511	0.404	0.475	-	0.290	63.8	19.9
cgRNASP-PC	0.092	-	0.525	0.384	0.414	-	0.266	56.1	25.7
cgRNASP-C	0.096	-	0.524	0.393	0.438	-	0.279	56.9	25.7
rsRNASP	0.023	-	0.434	0.446	<u>0.573</u>	-	0.347	64.0	19.6
Ideal value	1	1	1	1	1	1	1	73.8	7.7

Supplementary Table 5. Performance on 42 CASP16 targets. Values in **bold** indicate the best performance, while those with <u>underlines</u> represent the second-best. AUC was calculated on the overall data with an lDDT$_{RNA}$ cutoff of 75 to differentiate between 'good' and 'bad' decoys. $\rho_{\text{lDDT(Global)}}$, $\rho_{\text{lDDT(Local)}}$ and ρ_{RMSD} represent the Spearman correlation between the assessment scores and the true global lDDT$_{RNA}$, local lDDT$_{RNA}$, and RMSD, respectively. All correlation values are reported as absolute values.

Method	Overall				Per-target average				
	$\rho_{\text{lDDT(Global)}}$	$\rho_{\text{lDDT(Local)}}$	ρ_{RMSD}	AUC	$\rho_{\text{lDDT(Global)}}$	$\rho_{\text{lDDT(Local)}}$	ρ_{RMSD}	top 1 lDDT$_{RNA}$	top 1 RMSD(Å)
RNArank	**0.778**	**0.507**	0.722	**0.934**	0.549	**0.421**	**0.385**	**60.0**	**25.8**
lociPARSE	0.458	<u>0.386</u>	0.234	<u>0.658</u>	**0.597**	<u>0.393</u>	<u>0.283</u>	<u>58.9</u>	<u>26.2</u>
RNA3DCNN	0.252	0.253	0.019	0.584	0.478	0.298	0.175	51.7	32.0
DFIRE-RNA	<u>0.503</u>	-	**0.751**	0.230	0.531	-	0.201	57.5	29.6
cgRNASP	0.465	-	0.726	0.260	0.511	-	0.204	56.1	29.6
cgRNASP-PC	0.479	-	0.739	0.241	0.483	-	0.179	56.4	29.6
cgRNASP-C	0.490	-	<u>0.751</u>	0.241	0.485	-	0.161	51.8	31.9
rsRNASP	0.427	-	0.699	0.274	<u>0.549</u>	-	0.214	54.1	29.5
Ideal value	1	1	1	1	1	1	1	66.2	18.2

Supplementary Table 6. Performance on 17 nonredundant T24 targets. Values in **bold** indicate the best performance, while those with <u>underlines</u> represent the second-best. AUC was calculated on the overall data with an lDDT$_{RNA}$ cutoff of 75 to differentiate between 'good' and 'bad' decoys. $\rho_{lDDT(Global)}$，$\rho_{lDDT(Local)}$ and ρ_{RMSD} represent the Spearman correlation between the assessment scores and the true global lDDT$_{RNA}$, local lDDT$_{RNA}$, and RMSD, respectively. All correlation values are reported as absolute values.

Method	Overall				Per-target average				
	$\rho_{lDDT(Global)}$	$\rho_{lDDT(Local)}$	ρ_{RMSD}	AUC	$\rho_{lDDT(Global)}$	$\rho_{lDDT(Local)}$	ρ_{RMSD}	top 1 lDDT$_{RNA}$	top 1 RMSD(Å)
RNArank	**0.934**	**0.864**	**0.806**	**0.939**	**0.925**	**0.840**	**0.805**	**79.8**	**10.2**
lociPARSE	0.276	<u>0.286</u>	0.145	<u>0.848</u>	0.270	0.268	0.108	<u>74.5</u>	<u>10.9</u>
RNA3DCNN	<u>0.405</u>	0.283	0.196	0.818	0.432	<u>0.314</u>	0.276	52.5	16.5
DFIRE-RNA	0.096	-	<u>0.268</u>	0.662	0.637	-	0.500	66.3	14.4
cgRNASP	0.181	-	0.162	0.691	0.640	-	0.493	65.4	14.7
cgRNASP-PC	0.133	-	0.210	0.644	0.621	-	<u>0.512</u>	63.9	15.7
cgRNASP-C	0.217	-	0.146	0.690	<u>0.642</u>	-	0.489	65.2	14.7
rsRNASP	0.346	-	0.033	0.760	0.623	-	0.469	67.4	14.1
Ideal value	1	1	1	1	1	1	1	90.4	2.2

Supplementary Table 7. Performance on 10 nonredundant CASP15 targets. Values in **bold** indicate the best performance, while those with <u>underlines</u> represent the second-best. AUC was calculated on the overall data with an lDDT$_{RNA}$ cutoff of 75 to differentiate between 'good' and 'bad' decoys. $\rho_{lDDT(Global)}$，$\rho_{lDDT(Local)}$ and ρ_{RMSD} represent the Spearman correlation between the assessment scores and the true global lDDT$_{RNA}$, local lDDT$_{RNA}$, and RMSD, respectively. All correlation values are reported as absolute values.

Method	Overall				Per-target average				
	$\rho_{lDDT(Global)}$	$\rho_{lDDT(Local)}$	ρ_{RMSD}	AUC	$\rho_{lDDT(Global)}$	$\rho_{lDDT(Local)}$	ρ_{RMSD}	top 1 lDDT$_{RNA}$	top 1 RMSD(Å)
RNArank	**0.680**	**0.583**	**0.644**	**0.914**	**0.579**	**0.565**	**0.440**	**67.8**	**14.1**
lociPARSE	<u>0.485</u>	<u>0.504</u>	0.162	0.681	0.535	<u>0.413</u>	0.269	63.7	18.4
RNA3DCNN	0.231	0.316	0.031	<u>0.700</u>	0.200	0.238	0.040	36.1	32.3
DFIRE-RNA	0.035	-	<u>0.522</u>	0.415	0.502	-	<u>0.334</u>	63.7	17.2
cgRNASP	0.002	-	0.487	0.443	0.459	-	0.267	66.5	16.7
cgRNASP-PC	0.024	-	0.506	0.420	0.398	-	0.250	60.7	23.2
cgRNASP-C	0.027	-	0.502	0.431	0.420	-	0.256	60.0	24.1
rsRNASP	0.100	-	0.408	0.484	<u>0.565</u>	-	0.324	<u>67.4</u>	<u>15.6</u>
Ideal value	1	1	1	1	1	1	1	74.1	7.7

Supplementary Table 8. Performance on 28 nonredundant CASP16 targets. Values in **bold** indicate the best performance, while those with <u>underlines</u> represent the second-best. AUC was calculated on the overall data with an $lDDT_{RNA}$ cutoff of 75 to differentiate between 'good' and 'bad' decoys. $\rho_{lDDT(Global)}$, $\rho_{lDDT(Local)}$ and ρ_{RMSD} represent the Spearman correlation between the assessment scores and the true global $lDDT_{RNA}$, local $lDDT_{RNA}$, and RMSD, respectively. All correlation values are reported as absolute values.

Method	Overall				Per-target average				
	$\rho_{lDDT(Global)}$	$\rho_{lDDT(Local)}$	ρ_{RMSD}	AUC	$\rho_{lDDT(Global)}$	$\rho_{lDDT(Local)}$	ρ_{RMSD}	top 1 $lDDT_{RNA}$	top 1 RMSD(Å)
RNArank	**0.766**	**0.497**	0.698	**0.941**	0.535	**0.408**	**0.352**	**58.5**	<u>27.9</u>
lociPARSE	<u>0.545</u>	<u>0.434</u>	0.222	<u>0.680</u>	**0.629**	<u>0.407</u>	<u>0.276</u>	58.0	**27.3**
RNA3DCNN	0.306	0.275	0.007	0.592	0.517	0.304	0.175	49.6	34.5
DFIRE-RNA	0.452	-	<u>0.773</u>	0.176	0.556	-	0.204	<u>58.1</u>	31.2
cgRNASP	0.420	-	0.758	0.197	0.536	-	0.209	55.5	30.5
cgRNASP-PC	0.429	-	0.764	0.182	0.517	-	0.197	55.7	30.8
cgRNASP-C	0.440	-	**0.777**	0.188	0.507	-	0.164	49.9	32.8
rsRNASP	0.381	-	0.737	0.210	<u>0.567</u>	-	0.206	52.4	30.3
Ideal value	1	1	1	1	1	1	1	65.2	19.9

Supplementary Table 9. Results for ablation study on T24 Targets. Values in **bold** indicate the best performance, while those with underlines represent the second-best. AUC was calculated on the overall data with an lDDT$_{RNA}$ cutoff of 75 to differentiate between 'good' and 'bad' decoys. $\rho_{lDDT(Global)}$, $\rho_{lDDT(Local)}$ and ρ_{RMSD} represent the Spearman correlation between the assessment scores and the true global lDDT$_{RNA}$, local lDDT$_{RNA}$, and RMSD, respectively. All correlation values are reported as absolute values.

| Method	Overall				Per-target average				
	$\rho_{lDDT(Global)}$	$\rho_{lDDT(Local)}$	ρ_{RMSD}	AUC	$\rho_{lDDT(Global)}$	$\rho_{lDDT(Local)}$	ρ_{RMSD}	top 1 lDDT$_{RNA}$	top 1 RMSD(Å)
RNArank	**0.949**	**0.879**	0.832	<u>0.951</u>	**0.936**	**0.865**	<u>0.821</u>	<u>83.6</u>	<u>7.9</u>
w/o distance	0.938	0.847	0.817	0.944	0.922	0.838	0.810	76.7	10.0
w/o USR	<u>0.946</u>	<u>0.869</u>	**0.837**	**0.956**	0.926	<u>0.857</u>	**0.824**	**83.8**	**7.3**
w/o energy	0.941	0.862	0.813	0.950	<u>0.926</u>	0.855	0.805	81.8	8.2
w/o voxelization	0.930	0.850	<u>0.834</u>	0.936	0.909	0.837	0.802	74.0	11.6
Ideal value	1	1	1	1	1	1	1	94.6	1.9

Supplementary Table 10. Results for ablation study on CASP15 Targets. Values in **bold** indicate the best performance, while those with underlines represent the second-best. AUC was calculated on the overall data with an lDDT$_{RNA}$ cutoff of 75 to differentiate between 'good' and 'bad' decoys. $\rho_{lDDT(Global)}$, $\rho_{lDDT(Local)}$ and ρ_{RMSD} represent the Spearman correlation between the assessment scores and the true global lDDT$_{RNA}$, local lDDT$_{RNA}$, and RMSD, respectively. All correlation values are reported as absolute values.

Method	Overall				Per-target average				
	$\rho_{lDDT(Global)}$	$\rho_{lDDT(Local)}$	ρ_{RMSD}	AUC	$\rho_{lDDT(Global)}$	$\rho_{lDDT(Local)}$	ρ_{RMSD}	top 1 lDDT$_{RNA}$	top 1 RMSD(Å)
RNArank	**0.706**	**0.589**	**0.686**	**0.915**	**0.552**	**0.536**	<u>0.395</u>	<u>67.0</u>	**14.3**
w/o distance	<u>0.658</u>	0.519	0.602	0.889	0.541	0.477	**0.396**	63.4	17.0
w/o USR	0.653	<u>0.535</u>	<u>0.657</u>	0.886	0.490	0.473	0.382	63.0	16.7
w/o energy	0.603	0.470	0.515	<u>0.909</u>	<u>0.552</u>	<u>0.484</u>	0.383	**67.8**	<u>14.9</u>
w/o voxelization	0.590	0.483	0.548	0.909	0.450	0.432	0.375	56.4	17.6
Ideal value	1	1	1	1	1	1	1	73.8	7.7

Supplementary Table 11. Results for ablation study on CASP16 Targets. Values in **bold** indicate the best performance, while those with underlines represent the second-best. AUC was calculated on the overall data with an lDDT$_{RNA}$ cutoff of 75 to differentiate between 'good' and 'bad' decoys. $\rho_{lDDT(Global)}$, $\rho_{lDDT(Local)}$ and ρ_{RMSD} represent the Spearman correlation between the assessment scores and the true global lDDT$_{RNA}$, local lDDT$_{RNA}$, and RMSD, respectively. All correlation values are reported as absolute values.

| Method	Overall				Per-target average				
	$\rho_{lDDT(Global)}$	$\rho_{lDDT(Local)}$	ρ_{RMSD}	AUC	$\rho_{lDDT(Global)}$	$\rho_{lDDT(Local)}$	ρ_{RMSD}	top 1 lDDT$_{RNA}$	top 1 RMSD(Å)
RNArank	**0.778**	**0.507**	<u>0.722</u>	<u>0.934</u>	**0.549**	**0.421**	**0.385**	**60.0**	**25.8**
w/o distance	0.718	0.449	0.665	0.925	0.465	0.373	0.348	56.8	27.5
w/o USR	<u>0.778</u>	<u>0.496</u>	**0.770**	**0.941**	<u>0.489</u>	<u>0.405</u>	<u>0.363</u>	57.8	26.8
w/o energy	0.591	0.428	0.456	0.882	0.466	0.401	0.344	<u>58.2</u>	<u>26.4</u>
w/o voxelization	0.631	0.379	0.677	0.921	0.323	0.316	0.313	57.3	26.8
Ideal value	1	1	1	1	1	1	1	66.2	18.2

Supplementary Table 12. Computational cost of RNArank on RNA decoys of varying lengths. Performance was benchmarked on our computing cluster, with each run allocated a single Intel(R) Xeon(R) Platinum 8260 CPU core and one NVIDIA A100-PCIE-40GB GPU. The analysis was conducted on the decoy set submitted for AF3-server group in CASP16. All reported values represent the mean ± standard deviation of 10 independent runs.

Length range (nt)	CPU feature extraction (s)	GPU inference (s)	Peak CPU memory (GB)	Peak GPU memory (GB)
50-100	1.89 ± 0.46	0.16 ± 0.02	1.69 ± 0.09	0.64 ± 0.04
100-300	5.48 ± 2.42	0.27 ± 0.11	1.77 ± 0.12	0.97 ± 0.18
300-600	25.09 ± 4.72	1.68 ± 0.33	2.30 ± 0.15	2.35 ± 0.27
600-850	41.89 ± 4.90	3.35 ± 0.56	2.83 ± 0.13	4.08 ± 0.60
All	16.87 ± 14.95	1.21 ± 1.15	2.10 ± 0.43	1.82 ± 1.23

Supplementary Figures
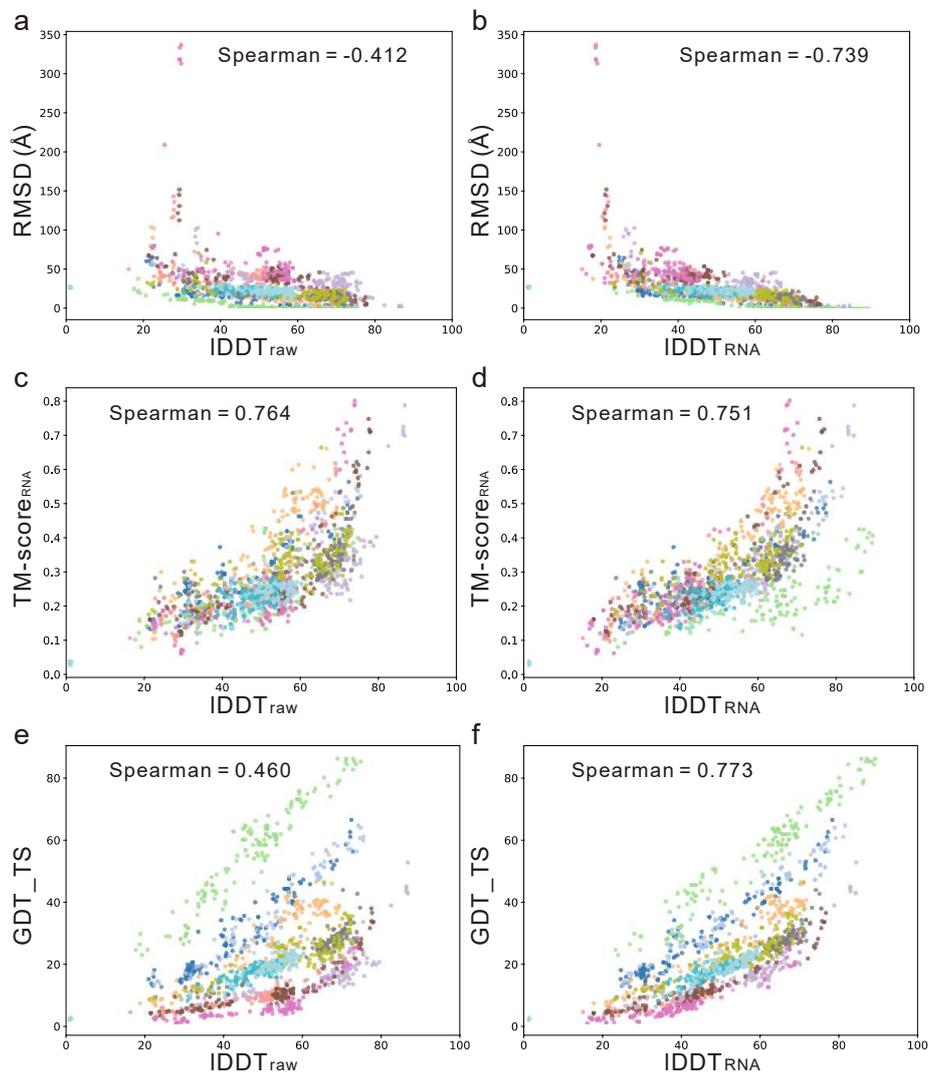
Supplementary Figure 1. Relationship between the two lDDT metrics and the other three established metrics for CASP15 targets. Each color corresponds to a target.
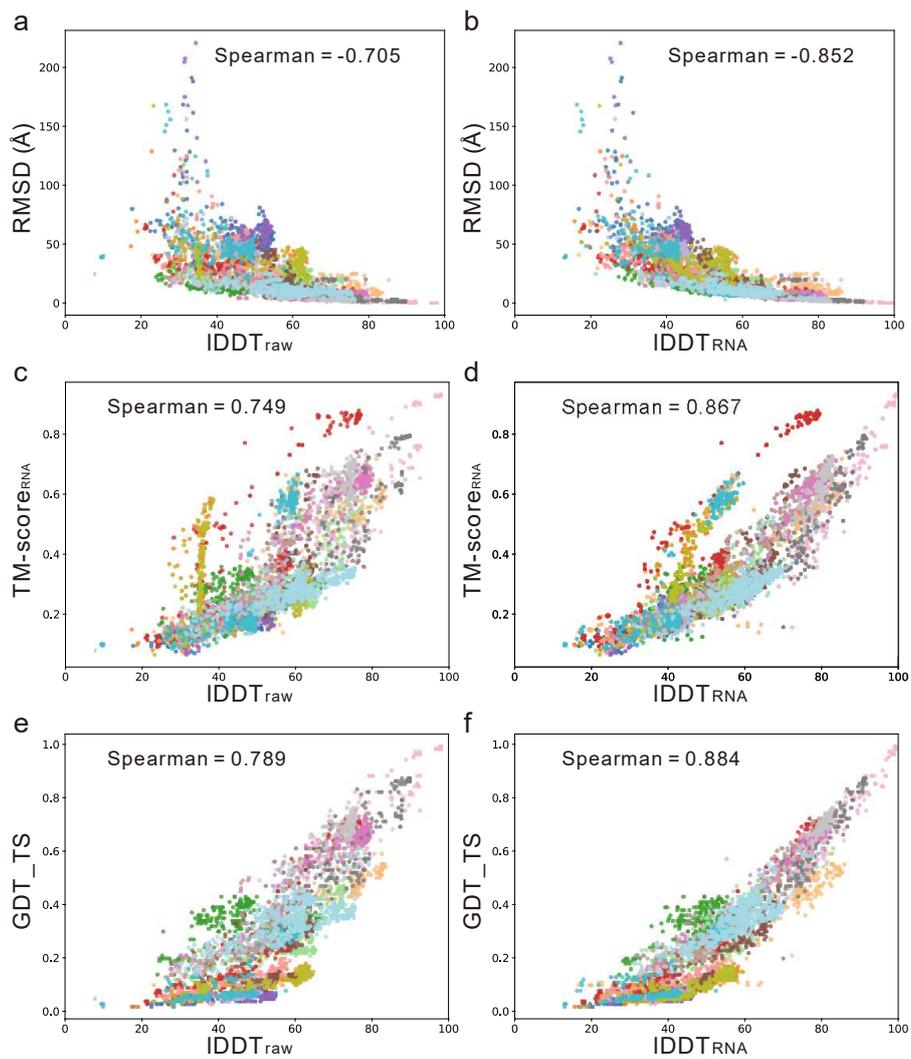
Supplementary Figure 2. Relationship between the two lDDT metrics and the other three established metrics for CASP16 targets. Each color corresponds to a target.
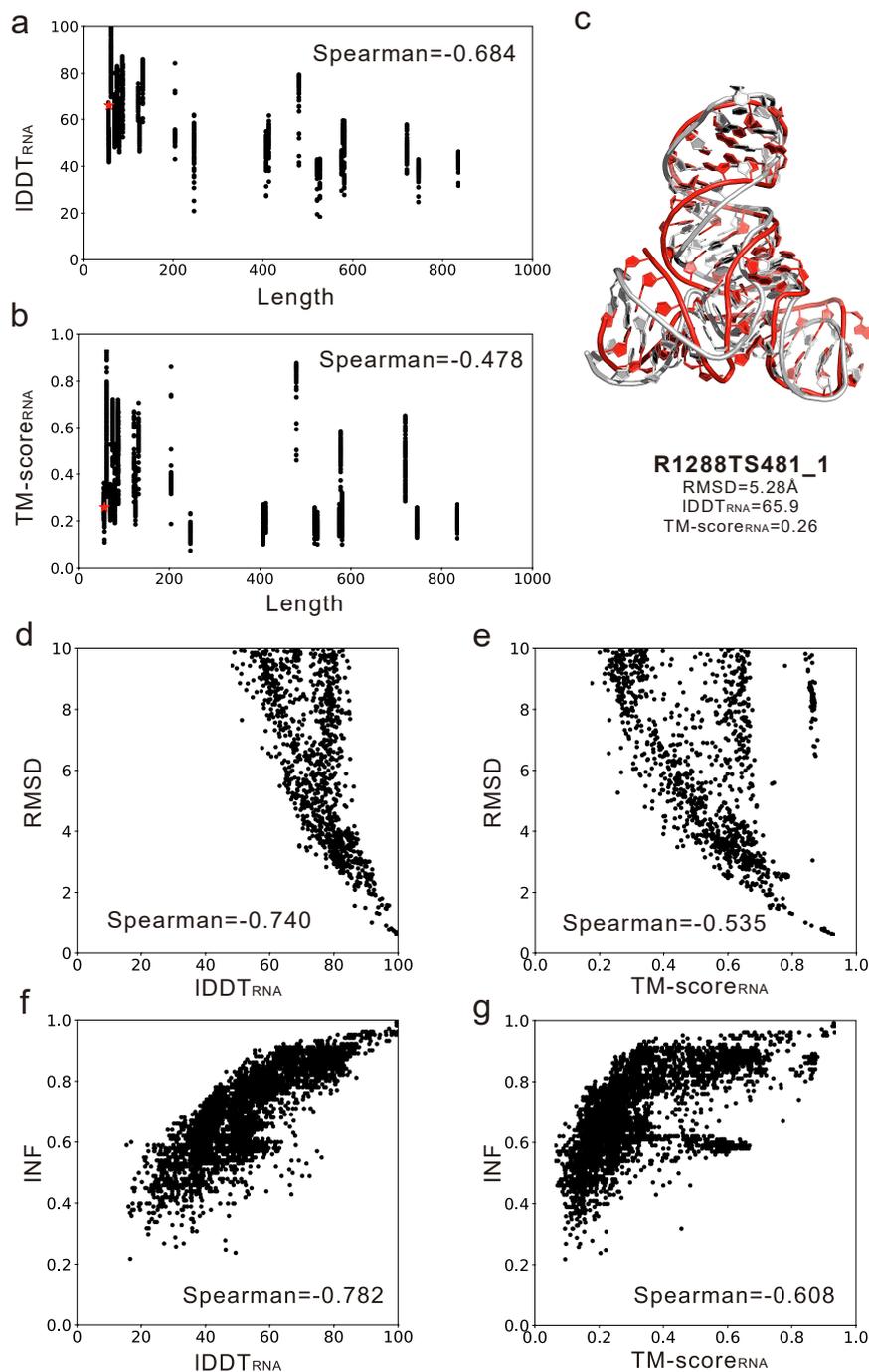
Supplementary Figure 3. Comparative analysis of lDDT$_{RNA}$ and TM-score$_{RNA}$ for RNA model quality assessment on the CASP16 dataset. (a, b) The relationship between the ground-truth scores (lDDT$_{RNA}$ and TM-score$_{RNA}$) of decoy models and their corresponding target lengths. To mitigate the confounding effects of outliers, all decoys with an RMSD Z-score greater than 0 (i.e., above average) were excluded, resulting in a final sample size of n=4129 decoys. The red stars highlight the model R1288TS481_1. **(c)** Superimposition of R1288TS481_1 (red) onto the experimental structure of R1288 (gray). **(d, e)** The relationship between RMSD and the quality scores for decoys with RMSD < 10 Å. **(f, g)** The relationship between Interaction Network Fidelity (INF) and the quality scores for all decoys. Note that this analysis excluded 6 targets lacking official assessments.
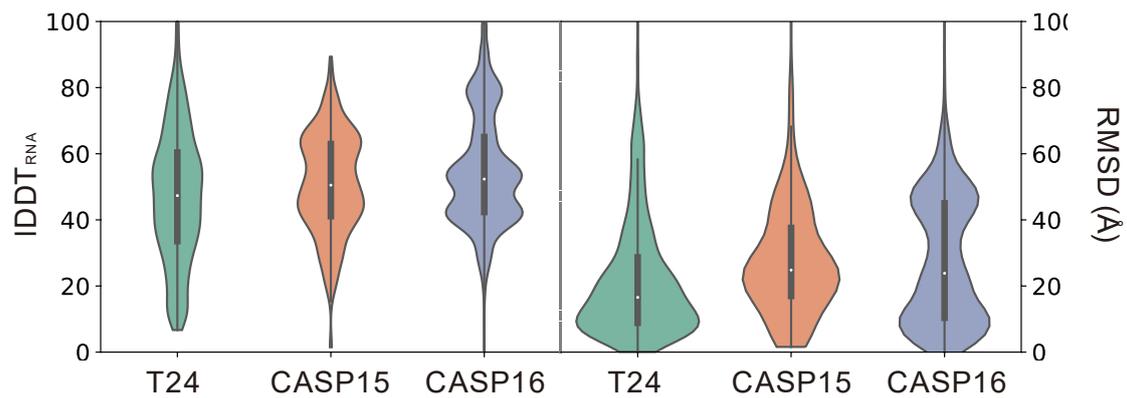
Supplementary Figure 4. Distributions of the ground-truth lDDT$_{RNA}$ and RMSD values on three benchmark sets. RMSD values are clipped to a maximum of 100 Å for better visualization. Data distributions were derived from n=2837 (T24), n=1623 (CASP15), and n=6678 (CASP16) independent structural models.
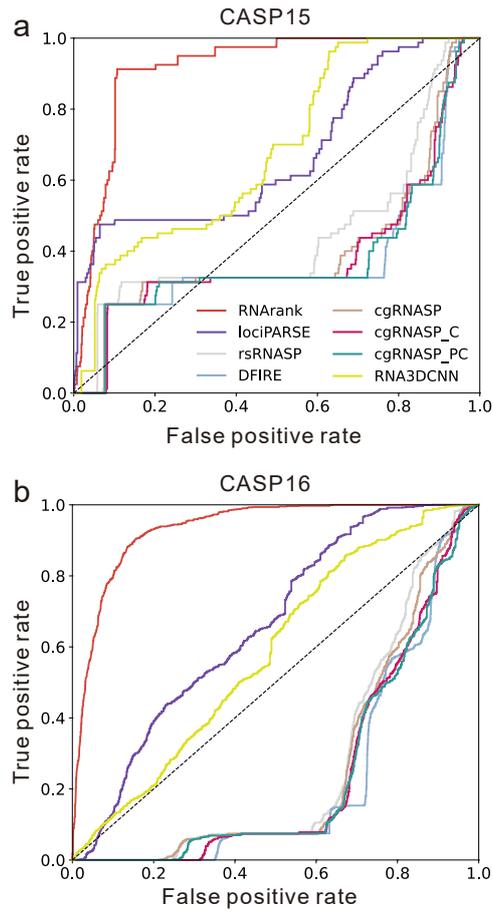
Supplementary Figure 5. ROC curves on two CASP datasets. (a) CASP15 dataset. **(b)** CASP16 dataset.
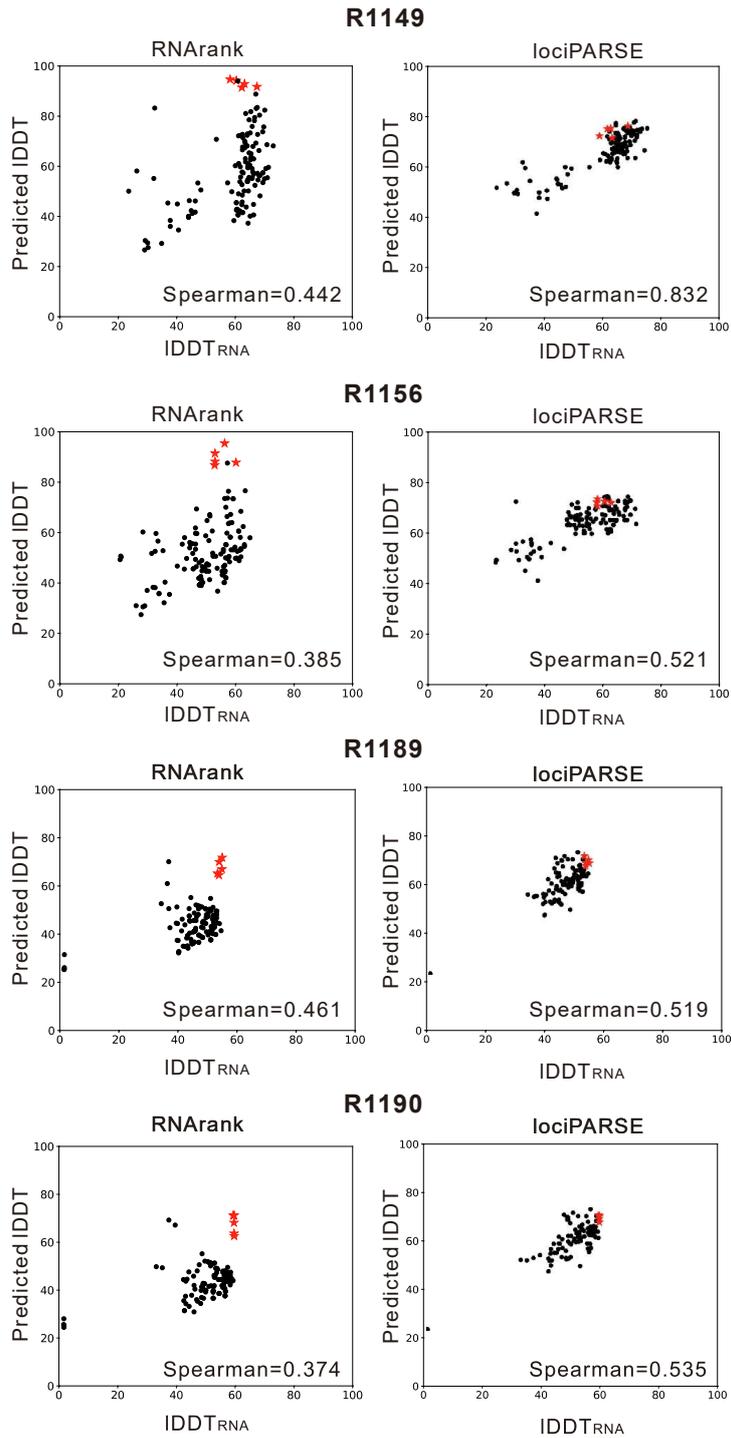
Supplementary Figure 6. Real lDDT$_{RNA}$ vs. predicted scores on four CASP15 targets. The red stars highlight the TS081 models.
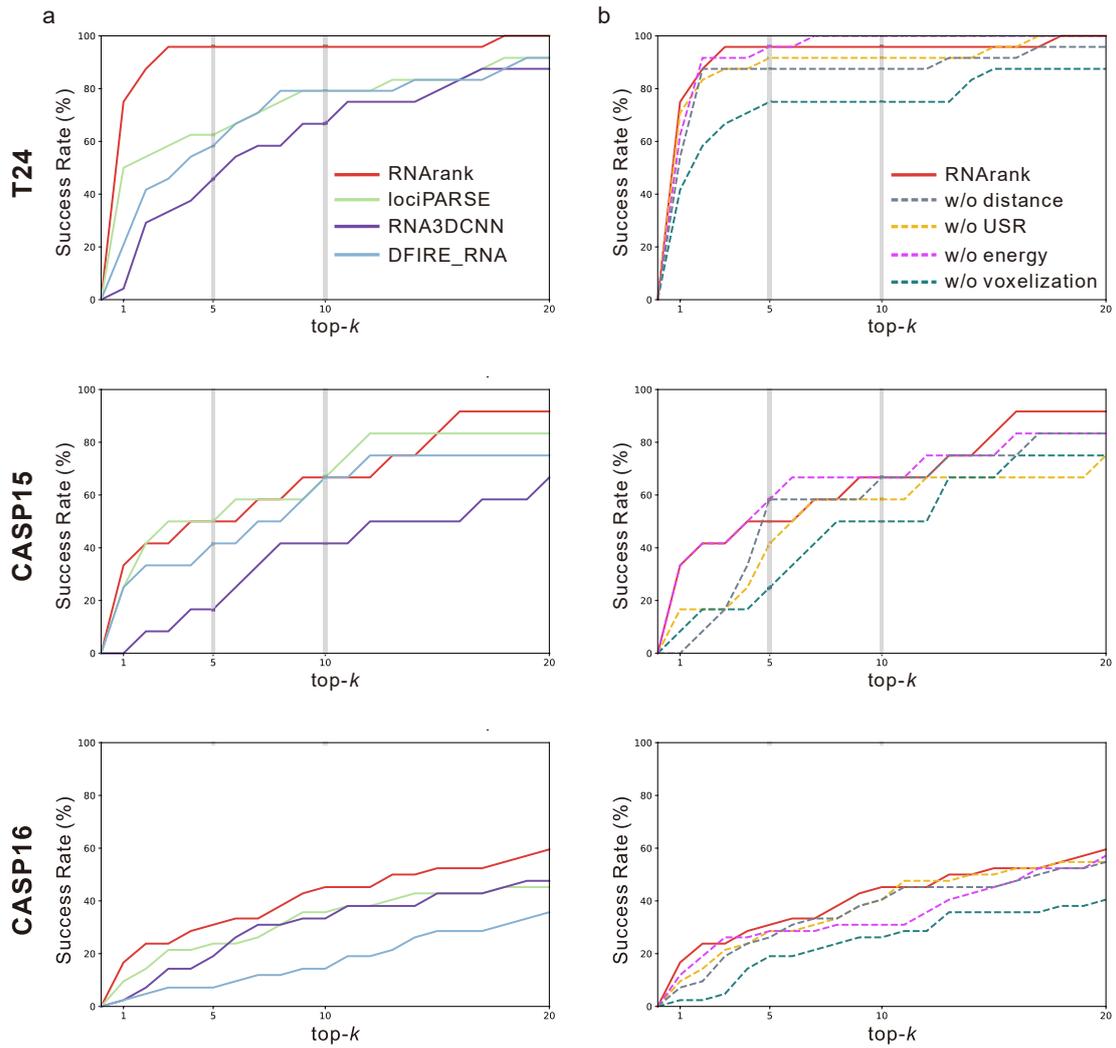
Supplementary Figure 7. Success rate within the top-*k* ranked decoys on three benchmark sets. A prediction for a given target is defined as "success" if at least one of the true top-5 best decoys (as measured by lDDT$_{RNA}$) is present within the top-*k* models ranked by the assessment method. **(a)** The comparison against other methods. **(b)** The results of the ablation study.
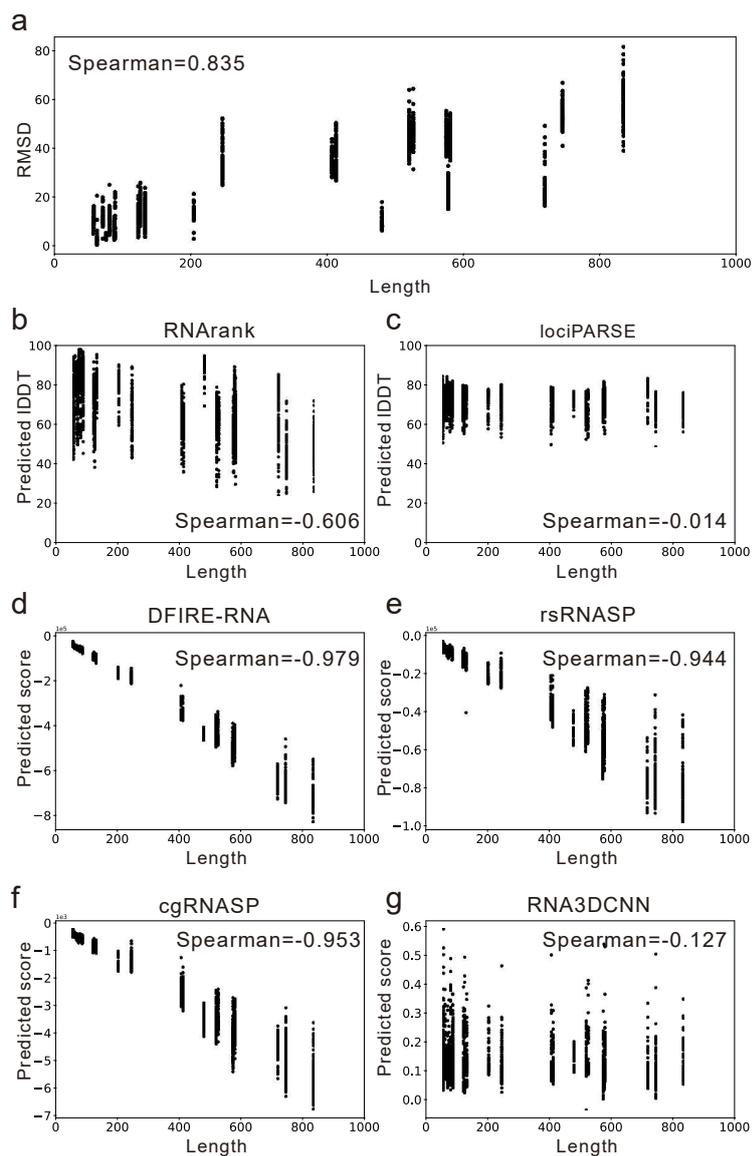
Supplementary Figure 8. Length-dependency analysis of different scores on the CASP16 dataset. (a) The relationship between the ground-truth RMSD of decoy models and target length. **(b-g)** The relationship between the quality scores predicted by various methods and the target length. To minimize the impact of outliers, decoys with a lDDT$_{RNA}$ Z-score less than 0 (i.e., below average) were excluded from all panels, resulting in a final sample size of n=4213 decoys.
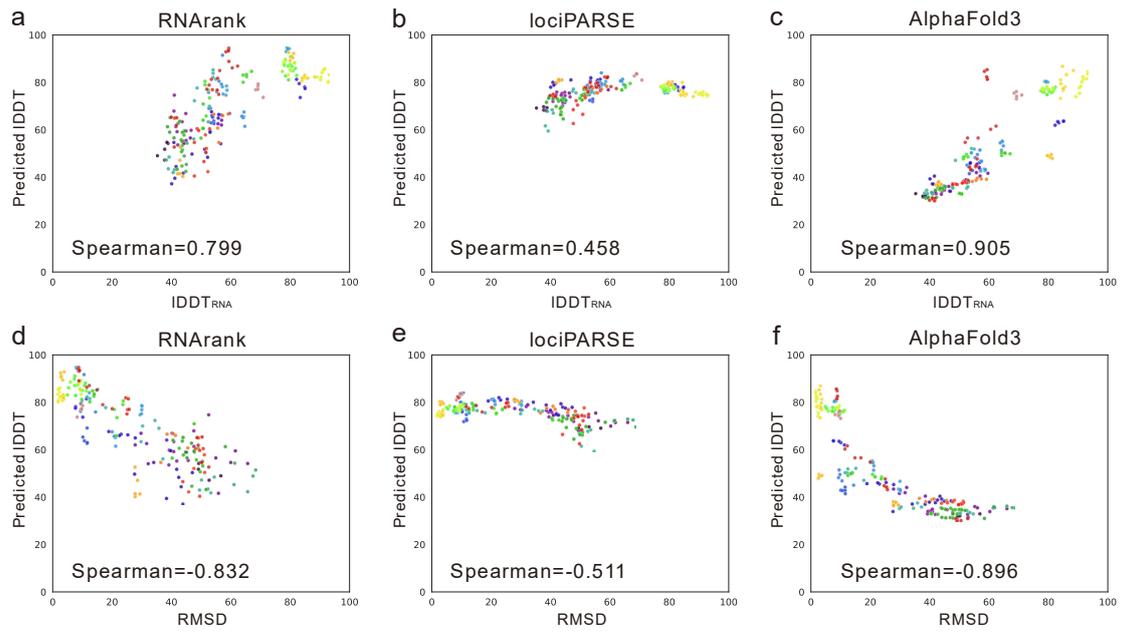
Supplementary Figure 9. Comparison of RNArank with AlphaFold3's self-assessment on CASP16 AlphaFold3 models. Each point represents an AlphaFold3 model, with its color indicating the corresponding source target.
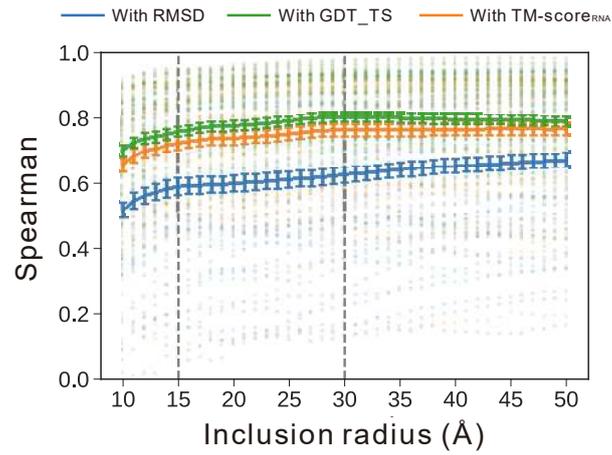
Supplementary Figure 10. Per-target average correlation profiles between lDDT$_{RNA}$ (with different inclusion radius) and three established global metrics on the combined CASP sets (n=7508 independent structural decoys, excluding 6 CASP16 targets lacking official assessments). Error bars represent 10% of the standard deviation. All correlation values are reported as absolute values.
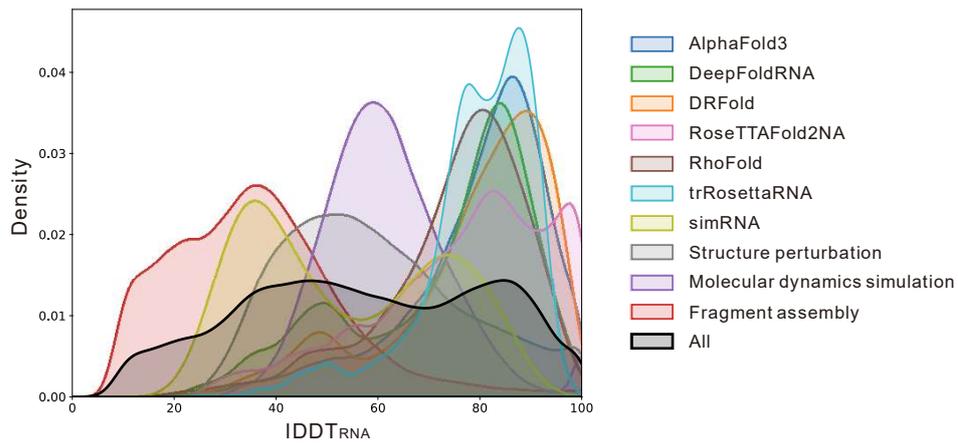
Supplementary Figure 11. Distribution of true lDDT$_{RNA}$ scores in the training set grouped by decoy generation method. The distribution is derived from a total of n=220407 independent structural models, including: Fragment assembly (n=80489), Structure perturbation (n=32523), Molecular Dynamics (n=29278), AlphaFold3 (n=19106), DeepFoldRNA (n=15057), RoseTTAFold2NA (n=13326), DRFold (n=13057), trRosettaRNA (n=12590), RhoFold (n=3346), and simRNA (n=1635).

Supplementary References

1   Ballester, P. J., Finn, P. W. & Richards, W. G. Ultrafast shape recognition: Evaluating a new ligand-based virtual screening technology. *Journal of Molecular Graphics and Modelling* **27**, 836-845, doi:https://doi.org/10.1016/j.jmgm.2009.01.001 (2009).

2   Guo, S. S., Liu, J., Zhou, X. G. & Zhang, G. J. DeepUMQA: ultrafast shape recognition-based protein model quality assessment using deep learning. *Bioinformatics* **38**, 1895-1903, doi:10.1093/bioinformatics/btac056 (2022).

3   Li, J. *et al.* RNA3DCNN: Local and global quality assessments of RNA 3D structures using 3D deep convolutional neural networks. *PLOS Computational Biology* **14**, e1006514, doi:10.1371/journal.pcbi.1006514 (2018).

4   Abramson, J. *et al.* Accurate structure prediction of biomolecular interactions with AlphaFold 3. *Nature* **630**, 493-500, doi:10.1038/s41586-024-07487-w (2024).

5   Pearce, R., Omenn, G. S. & Zhang, Y. De Novo RNA Tertiary Structure Prediction at Atomic Resolution Using Geometric Potentials from Deep Learning. *bioRxiv*, 2022.2005.2015.491755, doi:10.1101/2022.05.15.491755 (2022).

6   Li, Y. *et al.* Integrating end-to-end learning with deep geometrical potentials for ab initio RNA structure prediction. *Nat Commun* **14**, 5745, doi:10.1038/s41467-023-41303-9 (2023).

7   Shen, T. *et al.* Accurate RNA 3D structure prediction using a language model-based deep learning approach. *Nat Methods* **21**, 2287-2298, doi:10.1038/s41592-024-02487-0 (2024).

8   Popenda, M. *et al.* Automated 3D structure composition for large RNAs. *Nucleic Acids Res* **40**, e112, doi:10.1093/nar/gks339 (2012).

9   Sarzynska, J., Popenda, M., Antczak, M. & Szachniuk, M. RNA tertiary structure prediction using RNAComposer in CASP15. *Proteins* **91**, 1790-1799, doi:10.1002/prot.26578 (2023).

10   Baek, M. *et al.* Accurate prediction of protein-nucleic acid complexes using RoseTTAFoldNA. *Nat Methods* **21**, 117-121, doi:10.1038/s41592-023-02086-5 (2024).

11   Wang, W. *et al.* trRosettaRNA: automated prediction of RNA 3D structure with transformer network. *Nat Commun* **14**, 7266, doi:10.1038/s41467-023-42528-4 (2023).

12   Boniecki, M. J. *et al.* SimRNA: a coarse-grained method for RNA folding simulations and 3D structure prediction. *Nucleic Acids Res* **44**, e63, doi:10.1093/nar/gkv1479 (2016).